Cascaded Model Predictive Control of Six-phase Permanent Magnet Synchronous Motor with Fault Tolerant Ability

Ling Feng, Zhaohui Wang, Jianghua Feng, and Wensheng Song, *Senior Member*, *IEEE*

***Abstract*—In the field of high-power electric drives, multiphase motors have the advantages of high power-density, excellent fault tolerance and control flexibility. But their decoupling control and modulation process are much more complicated compared with three-phase motors due to the increased degree of freedom. Finite control set model predictive control can reduce the difficulties of controlling six-phase motors because it does not require modulation process. In this paper, a cascaded model predictive control strategy is proposed for the optimal control of high-power six-phase permanent magnet synchronous motors. Firstly, the current prediction model of torque and harmonic subspaces are established by decoupling the six-phase spatial variables. Secondly, a cascaded cost function with fault-tolerant capability is proposed to eliminate the weighting factor in the cost function. And finally, the proposed strategy is demonstrated through theoretical analysis and experiments. It is validated that the proposed method is able to maintain excellent steady-state control accuracy and fast dynamic response while significantly reduce the control complexity of the system. Besides, it can easily achieve fault-tolerant operation under open-phase fault.**

***Index Terms*—Fault-tolerant control, Model predictive control, Permanent magnet synchronous motor, Six-phase motor, Weighting factor.**

I. Introduction

COMPARED with traditional three-phase motors, multi-phase permanent magnet synchronous motors (PMSM) attract more and more attention in high-power AC drive fields such as aerospace, naval propulsion and rail transportation because of their high efficiency, power density and control flexibility [1]-[3]. Due to the increased number of phases, the vector space of multiphase motor is quite complex. For example, the two-level six-phase inverter system has 64 voltage vectors, which requires a very complicated modulation process.

In order to simplify the control of multiphase inverter system, many researchers have adopted Model Predictive Control (MPC) as an upgrade of traditional control methods [4]-[9]. The Finite Control Set Model Predictive Control (FCS-MPC) makes full use of the discontinuous nature of the power electronic devices and can eliminate the complex modulation process. Compared with the traditional linear controller with space vector pulse width modulation (SVPWM) structure, MPC has many advantages. Firstly, its concept is simple and the optimal solution process is more in line with the decision mechanism of human brains. Secondly, it is easy to include nonlinear constraints, such as low switching frequency, low loss and output current distortion constraints. [7] provides the current prediction model for six-phase motor and implements single-step model prediction current control of a multiphase motor. [8] uses a model predictive controller to control a multiphase motor with fixed switching frequency. [9] introduces dead-beat model predictive algorithm and virtual voltage vector into a two-level six-phase inverter system. The virtual vectors proposed in [8] and [9] can achieve error-free tracking of flux and torque in the torque subspace while ensuring their projection on the harmonic subspace cancel each other. In summary, MPC provides a more novel and simple idea for optimal control of multiphase motors with guaranteed system performance.

The construction of cost function and selection of weighting factors are the key points of MPC research, and there are few mature theories to refer to. Most of the applications have adopted empirical and statistical methods to select the optimal weighting factors [8], [10]-[12]. The virtual-vector-based model predictive six-phase asynchronous motor control proposed in [8] uses a cost function containing four weighting factors. [10] proposes a model predictive torque control of a cascaded dual three-phase PMSM with also four weighting factors and both of them do not provide the selection method of weighting factors. Based on the dead-beat control strategy, the number of weighting factors in the cost function can be reduced. [11] constructs a cost function containing only the current components on harmonic subspace. [12] eliminates the weighting factors from the cost function which simply contains only the deviation component of the voltage. [13] uses the idea of dead-beat direct flux control to eliminate the weighting factor. Although these methods simplify the cost function, they all involve the solution of transcendental equations and other time-consuming algorithms, which increases the complexity of the control system. In [14], the cascaded cost function of three-phase motor is proposed for the first time, in which two

Manuscript received October 07, 2021; revised January 05, 2022, and April 02, 2022; accepted June 16, 2022. Date of publication September 25, 2023; date of current version June 08, 2023.

Ling Feng and Jianghua Feng are with CRRC ZhuZhou Institute Co., Ltd. ZhuZhou 412001, China (e-mail: feng_ling@foxmail.com).

Zhaohui Wang and Wensheng Song are with the School of Electrical Engineering, Southwest Jiaotong University, Chengdu 611756, China.

(Corresponding Author: Ling Feng)

Digital Object Identifier 10.30941/CESTEMS.2023.00033

vectors that satisfy the minimum torque error are selected first, and then the one that minimizes the flux tracking error is selected as the optimal vector. [15] proposed a generalized cascaded MPC of three-phase motor based on [14] by increasing the candidate vectors in the first step and demonstrating through simulation and experiment that the cascaded approach can successfully eliminate the weighting factors.

Fault-tolerant control is another key point of multiphase motor control, and at present most of the researches on this topic are based on the method of harmonic injection method [16]-[18]. The reference current is revised under different optimization constrains after fault, such as minimum copper loss, minimum peak current or minimum torque pulsation. And the PI with SPWM modulation is used to track the revised reference current. However, this method suffers with high output current ripple and low DC voltage utilization. In addition, it requires sensing the specific opened phase and constructing the reduced-dimension mathematical model. As different open phase corresponds to different decoupling transformation matrices separately. This makes the traditional fault tolerant control lack of practical application in inverter systems with high real-time requirements.

Compared with the traditional method, MPC has greater advantages in fault-tolerant control of multiphase motors. [19] proposes fault-tolerant control of a five-phase induction motor under phase open fault based on direct torque MPC with virtual vectors. The proposed method requires the construction of virtual vector space after phase loss and sensing the specific opened phase. [20] proposes a FCS-MPC method for open phase tolerant control of three-phase four-winding motor. But the proposed method also requires phase open detection and is not applicable to six-phase inverter system. [21] establishes fault-tolerant predictive control for a five-phase asynchronous motor based on a post-fault system predictive model, but the cost function is too complicated with four weighting factors. [22] proposes fault-tolerant predictive control of a six-phase PMSM based on pulse-width modulation. A dead-beat algorithm is adopted to calculate the reference vector which is then synthesized by the fundamental vectors. However, it is not suitable for application to high-power systems with low switching frequency, as the virtual vectors increase the switching frequency. [23] proposes a fault-tolerant model predictive control for PMSM with dual inverters supply, in order to construct a new voltage vector space, the decoupling matrix needs to be switched before and after fault, which increases the control complexity.

Inspired by the cascaded MPC proposed in [14], this paper proposes a cascaded model predictive current control strategy (CMPC) for the six-phase PMSM to eliminate the weighting factor in the cost function. Firstly, by decoupling the stator voltage and current into the torque, harmonic and circulating current subspaces, the current prediction models of the three subspaces are derived, and the cascaded cost functions of the torque and harmonic subspaces are constructed. Then, the CMPC and a traditional MPC method are compared both in static state and dynamic state. It is validated by the experiments that the CMPC can eliminate the influence of weighting factor on system performance and maintain satisfactory steady-state performance under different working conditions. Besides, the dynamic response of CMPC is comparable to that of the conventional current-tracking MPC. Last but not least, CMPC can achieve fault-tolerant operation in any open-phase condition without detection of specific faulty phase and switching control method.

II. Model of the System

A. State Variable Decoupling and Current Predictive Model

Fig. 1 shows the diagram of six-phase inverter system, the six-phase PMSM is designed with two sets of Y-connected windings phase shifted by 30 electrical degrees without connection between neutral points. The switching function of the six-phase is defined as $s_k = 0$ or $1 (k = 1, 2...6)$, where 0 represents lower switch on and 1 represents upper switch on. The relationship between switching function and the corresponding phase voltage can be derived as (1).

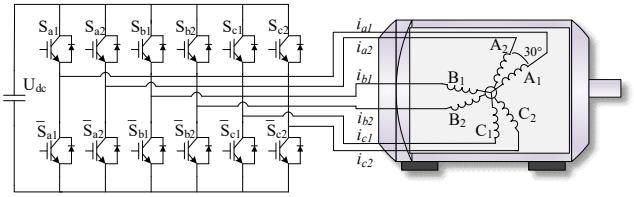

Fig. 1. Six-phase PMSM inverter system.

$$\begin{bmatrix} u_{a1} \\ u_{b1} \\ u_{c1} \\ u_{a2} \\ u_{b2} \\ u_{c2} \end{bmatrix} = \frac{U_{dc}}{3} \cdot \begin{bmatrix} 2 & -1 & -1 & 0 & 0 & 0 \\ -1 & 2 & -1 & 0 & 0 & 0 \\ -1 & -1 & 0 & 0 & 0 & 0 \\ 0 & 0 & 0 & 2 & -1 & -1 \\ 0 & 0 & 0 & -1 & 2 & -1 \\ 0 & 0 & 0 & -1 & -1 & 2 \end{bmatrix} \cdot \begin{bmatrix} S_{a1} \\ S_{b1} \\ S_{c1} \\ S_{a2} \\ S_{b2} \\ S_{c2} \end{bmatrix} \tag{1}$$

where u is the phase voltage, U_{dc} is the DC voltage and S is the switching state of the inverter.

By defining the 6×6 decoupling matrix M_D in (2), the phase voltage and current can be decoupled to three mutually perpendicular subspaces denoted as $\alpha-\beta$, z_1-z_2 and o_1-o_2, where the $\alpha-\beta$ torque subspace coincides with the rotation of air gap flux, the corresponding current component will form a rotating magnetic potential in the air gap and participate in the electromechanical energy conversion of the system. The current component of the harmonic subspace z_1-z_2 is not related to the electromechanical energy conversion but determines the harmonic component of the system. Due to the unconnected neutral points, the o_1-o_2 subspace component is 0. According to the system topology and switching function, the vector distribution in $\alpha-\beta$ and z_1-z_2 can be obtained as shown in Fig. 2. From the vector distribution, it can be seen that the 12 vectors with the largest projection amplitude in the $\alpha-\beta$ subspace have exactly the smallest projection in the z_1-z_2 subspace, which means these vectors can output the maximum torque component while ensuring the minimum current harmonic. The number of candidate vectors in six-phase

motor MPC can be reduced by selecting only 12 long vectors as candidate vectors which based on the same consideration in the conventional six-phase SVPWM.

$$\begin{bmatrix} u_\alpha \\ u_\beta \\ u_{z1} \\ u_{z2} \\ u_{o1} \\ u_{o1} \end{bmatrix} = \frac{1}{3}\cdot \begin{bmatrix} 1 & -\frac{1}{2} & -\frac{1}{2} & \frac{\sqrt{3}}{2} & -\frac{\sqrt{3}}{2} & 0 \\ 0 & \frac{\sqrt{3}}{2} & -\frac{\sqrt{3}}{2} & \frac{1}{2} & \frac{1}{2} & -1 \\ 1 & -\frac{1}{2} & -\frac{1}{2} & -\frac{\sqrt{3}}{2} & \frac{\sqrt{3}}{2} & 0 \\ 0 & -\frac{\sqrt{3}}{2} & \frac{\sqrt{3}}{2} & \frac{1}{2} & \frac{1}{2} & -1 \\ 1 & 1 & 1 & 0 & 0 & 0 \\ 0 & 0 & 0 & 1 & 1 & 1 \end{bmatrix} \cdot \begin{bmatrix} u_{a1} \\ u_{b1} \\ u_{c1} \\ u_{a2} \\ u_{b2} \\ u_{c2} \end{bmatrix} \quad (2)$$

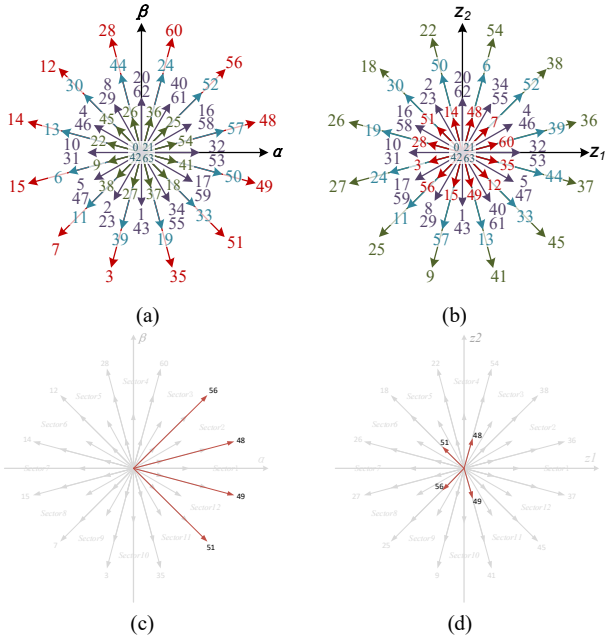

Fig. 2. Projection of voltage vector on (a) α-β torque subspace. (b) z_1-z_2 harmonic subspace. (c) projection of long vectors in α-β subspace. (d) projection of long vectors in z_1-z_2 subspace.

Taking the stator currents in the torque subspace and the harmonic subspace as the state space variables, the state equations of the system can be obtained by rotating and transforming the torque subspace variables to the dq coordinate system as (3)~(5).

$$\begin{bmatrix} u_d \\ u_q \end{bmatrix} = \begin{bmatrix} \cos\theta & -\sin\theta \\ \sin\theta & \cos\theta \end{bmatrix} \cdot \begin{bmatrix} u_\alpha \\ u_\beta \end{bmatrix} \quad (3)$$

$$\begin{cases} u_d = R_s i_d - \omega_r \Psi_q + L_d \dfrac{di_d}{dt} \\ u_q = R_s i_d - \omega_r \Psi_q + L_q \dfrac{di_q}{dt} \end{cases} \quad (4)$$

$$\begin{cases} u_{z1} = R_s i_{z1} + L_m \dfrac{di_{z1}}{dt} \\ u_{z2} = R_s i_{z2} + L_m \dfrac{di_{z2}}{dt} \end{cases} \quad (5)$$

Using the forward Euler method to discretize the above continuous state equations, the prediction model of stator current can be obtained as (6) and (7).

$$\begin{cases} i_d(k+1) = i_d(k)(1-\dfrac{R_s T_s}{L_d}) + \dfrac{T_s}{L_d}(u_d(k+1) + \omega_r L_d i_q(k)) \\ i_q(k+1) = i_q(k)(1-\dfrac{R_s T_s}{L_q}) + \dfrac{T_s}{L_q}(u_q(k+1) - \omega_r L_d i_d(k) - \omega_r \psi_r) \end{cases} \quad (6)$$

$$\begin{cases} i_{z1}(k+1) = (1-\dfrac{R_s T_s}{L_m}) i_{z1}(k) + \dfrac{T_s}{L_m} u_{z1}(k+1) \\ i_{z2}(k+1) = (1-\dfrac{R_s T_s}{L_m}) i_{z2}(k) + \dfrac{T_s}{L_m} u_{z2}(k+1) \end{cases} \quad (7)$$

where $u_x(x=d,q,z_1,z_2)$ is the stator voltage and $i_x(x=d,q,z_1,z_2)$ is the stator current; motor parameters $\psi_r, L_d, L_q, L_m, R_s$ are permanent magnet chain, stator inductance in dq coordinate system, mutual inductance and stator resistance, respectively; system parameters T_s and ω_r are sampling period and rotor speed.

B. Design of the Cost Function

A traditional current tracking six-phase motor MPC block diagram is shown in Fig. 3. The six-phase currents are decoupled to obtain the current components in $\alpha-\beta$ subspace and z_1-z_2 subspace at moment k, which are then substituted into the predictive model to obtain the predicted currents at moment k+1. The output of external loop is coordinately transformed to obtain the reference value of i_d^* and i_q^*. Under normal operating conditions, the reference value of z_1-z_2 is set as zero to reach zero harmonic current. According to the reference value, the candidate vectors are substituted into the cost function in turn, and the one that minimizes the error between predicted and reference value is selected as the optimum driving sequence named *k_opt*. In order to reduce the system switching frequency, four zero vectors are selected in addition to the 12 long vectors, so that in each prediction cycle, there are a total of 16 candidate vectors for current prediction.

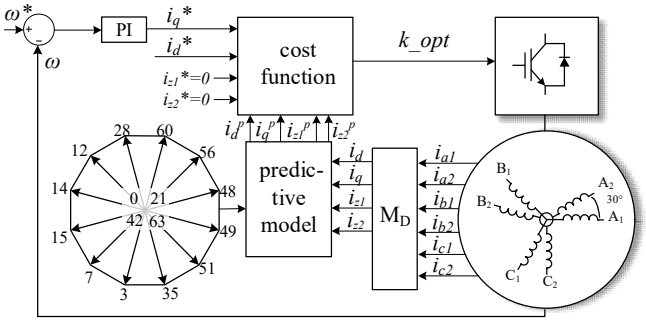

Fig. 3. Control diagram of conventional six-phase MPC.

The conventional cost function of current-tracking six-phase MPC is generally designed as (8).

$$g = [|i_d(k+1) - i_d^*| + |i_q(k+1) - i_d^*|] + \lambda[|i_{z1}(k+1)| + |i_{z2}(k+1)|] \quad (8)$$

The cost function contains two parts, and the importance of these two parts are regulated by the weighting factor λ. The first component is a penalty term for the tracking error in the torque subspace and the second component penalizes the tracking error in the harmonic subspace. The tracking error in

the torque and harmonic subspace can be balanced by adjusting the weighting factor λ. Under different working conditions, how to find the optimal weighting factor λ to balance the tracking error of the two parts is an important problem faced by the traditional six-phase MPC.

To solve this problem, the proposed CMPC in this paper is derived by splitting the traditional cost function (8) into (9) and (10).

$$g_1 = |i_d(k+1) - i_d^*| + |i_q(k+1) - i_q^*| \tag{9}$$

$$g_2 = |i_{z1}(k+1)| + |i_{z2}(k+1)| \tag{10}$$

The control diagram of CMPC constructed according to (9) and (10) is shown in Fig. 4. The difference between CMPC and the traditional MPC is that after the current reference in q-axis is derived from the external loop, the seven vectors with the smallest torque subspace tracking error are first selected as a new candidate vector set named as $\{k\_opt1\}$ through cost function (9). And then the vector that minimizes the harmonic subspace tracking error is selected from the seven candidates in $\{k\_opt1\}$ through cost function (10) as the optimal vector named *k_opt*. The use of two cascaded cost functions eliminates the weighting factor in (8), which can ensure smooth operation of the system under different operating conditions and avoid the imbalance between torque and harmonic subspaces current control caused by unreasonable design of the weighting factor.

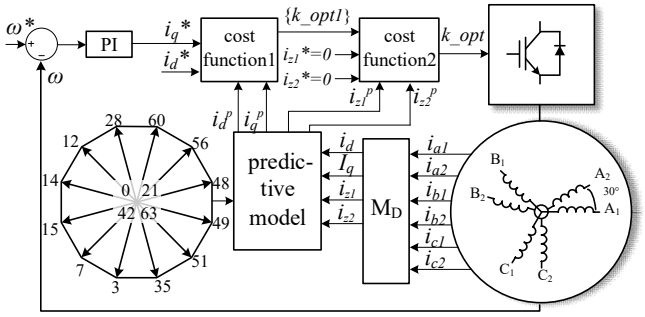

Fig. 4. Control diagram of the CMPC proposed in this paper.

III. Fault-tolerant Control of Six-phase Motors

Another advantage of the proposed CMPC is that it enables fault-tolerant control of a six-phase PMSM after any open phase fault without the need to detect the specific phase loss. The same decoupling matrix and cost function is used before and after fault, which can solve problems such as speed-torque pulsations and thus ensuring coherent operation before and after fault.

A. Fault-tolerant Operation under the Principle of Minimum Copper Loss

In motor drive systems, various open and short-circuit faults can be converted into open phase faults by measures such as hardware isolation and so on. So the faults discussed in this paper are open circuit of one inverter arm with no damage of the motor windings. It is assumed that the motor parameters do not change with the operating conditions. Without loss of generality, assume an open circuit fault occurs in c_2, the voltage, magnetic flux and torque equations of the system will not be affected, and the current equations will be reduced by one degree of freedom. From the decoupling matrix M_D in (2), we can see that i_α, i_{z1} are independent of the c_2 phase currents and therefore will not be influenced, while i_β and i_{z2} will be constrained by (11).

$$i_{c2} = -i_\beta - i_{z2} = 0 \tag{11}$$

According to (13), after a phase loss occurs, the fundamental and harmonic subspaces are no longer decoupled from each other. And the $z_1 - z_2$ harmonic subspace current will not be zero at this time. The traditional fault-tolerant control method is to apply constraints to the $z_1 - z_2$ current, and to perform closed-loop control of the $z_1 - z_2$ current according to different constraints such as minimum stator copper loss and maximum torque output, etc. The reference value of $z_1 - z_2$ will be different for different fault phase, so the specific opened phase needs to be detected first, which greatly increases the complexity of traditional fault-tolerant control. Taking the minimum stator copper loss constrain as an example, the regulated current references after different phase faults are shown in Table I.

TABLE I
REFERENCE FOR $z_1 - z_2$ SUBSPACE OF TRADITIONAL FAULT-TOLERANT CONTROL

Opend phase	Reference for z_1 axis	Reference for z_2 axis
a_1	$-i_\alpha$	0
a_2	i_α	0
b_1	0	i_β
b_2	i_α	0
c_1	0	i_β
c_2	0	$-i_\beta$

This problem can be solved simply and effectively by using the CMPC cost function construction proposed in this paper. The cascaded cost function consists of two parts. The first part controls the fundamental subspace current which can ensure the output torque remains unchanged before and after fault, and the second part controls the harmonic subspace current, which ensures the minimum stator copper loss before and after fault.

Under normal operation, the harmonic subspace reference value is zero, at which point the total stator copper loss of the six-phase motor can be expressed as:

$$P_{Cu} = i_s^T R_s i_s = 3R_s(i_\alpha^2 + i_\beta^2 + i_{z1}^2 + i_{z2}^2 + i_{o1}^2 + i_{o2}^2) \tag{12}$$

Since the output torque needs to remain constant during phase loss, i.e. the stator copper loss corresponding to the torque subspace is fixed, and the optimal conditions for the minimum stator copper loss constrain can be simplified as (13).

$$\min(i_{z1}^2 + i_{z2}^2 + i_{o1}^2 + i_{o2}^2) \tag{13}$$

As the current component in $o_1 - o_2$ subspace is 0, (13) can be further simplified as (14).

$$\min(i_{z1}^2 + i_{z2}^2) \tag{14}$$

(14) and (10) have the same physical meaning, from which it

can be seen that fault-tolerant control with minimum stator copper loss can be realized as long as the current of the z_1-z_2 subspace is minimized. Which is to say, after an open phase fault, fault-tolerant control with minimum stator copper loss can be achieved in an automatic way by keeping the structure of the cost function unchanged and still constraining the harmonic subspace current to zero. This is a feature that cannot be achieved by the traditional harmonic injection method.

The conventional fault-tolerant control requires different reference current of z_1-z_2 subspace for different phase loss. The CMPC fault-tolerant control proposed in this paper, on the other hand, unifies the reference of harmonic subspace and greatly simplifies the fault-tolerant control of six-phase motors.

IV. Experiment Verification

The CMPC method proposed in this paper is verified comparatively in the hardware in the loop (HIL) simulation platform shown in Fig. 5. Considering the excessive power of the real inverter and motor, the HIL verification based on DSP TMS320F28377D controller is adopted. The load consists of the FPGA-based simulated inverter, the PMSM motor and the tractor motor. System parameters are set as shown in Table II. The upper computer monitoring software stores and displays the sampling data at 10 kHz sampling frequency via Ethernet communication. The sampled stator current data is imported into PC for DFT analysis to obtain its total harmonic distortion (THD) value, while the output electromagnetic torque of the motor and the inverter switching frequency are transmitted to the upper computer for observation. The switching frequency is calculated from the average switching times of each phase per unit time. In addition, in order to reduce the influence of the external PI controller on the internal MPC controller, a tractor motor is adopted to make the controlled motor run at constant speed.

TABLE II
SYSTEM PARAMETERS

Symbol	Parameter	Quantity
R_S	Stator resistance	0.05 Ω
L_d	Stator inductance d-axis	3.3 mH
L_q	Stator inductance q-axis	3.3 mH
Ψ_R	Rotor flux	0.635 Wb
P	Pole pairs	4
P_{rated}	Rated power	190 kW
ω_{rated}	Rated speed	1500 rpm
f_{sw}	Control frequency	10 kHz
U_{DC}	DC voltage	1500 V

A. Steady State Performance

In order to verify the steady-state performance of CMPC and conventional current-tracking MPC under different working conditions, the steady-state performance comparison of these two strategies is carried out at constant speed of 1000 rpm. The experiment results are shown in Fig. 6 to Fig. 9 where from top to bottom are electromagnetic torque, current of $\alpha-\beta$ subspace, current of z_1-z_2 subspace and optimal vector number, respectively. Fig. 6 shows the experiment results of the traditional MPC at reference current of 1800 A. The weighting factor is selected as 3 after many tests. At this time, the torque

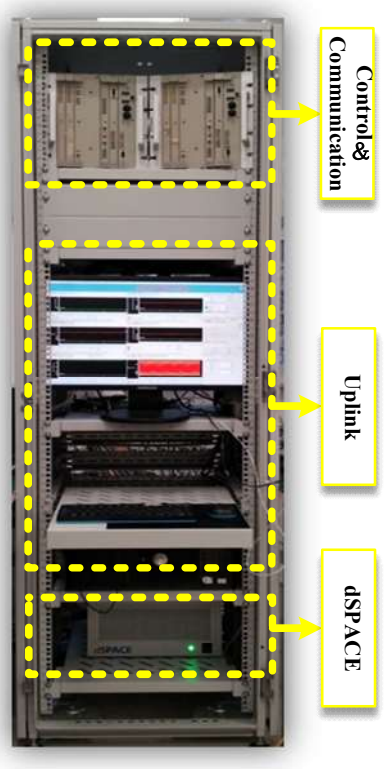

Fig. 5. The hardware in the loop simulation platform.

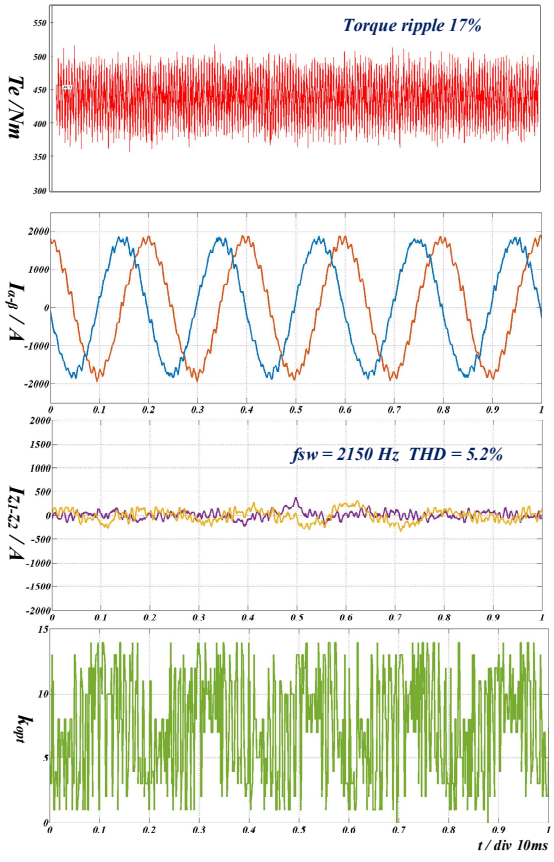

Fig. 6. Static performance of the traditional MPC of reference current 1800 A.

pulsation is 17%, the average switching frequency is 2150 Hz, and the THD of stator current is 5.2%.

It should be emphasized at first that the currents shown in the

experiment results are the $\alpha-\beta$ and z_1-z_2 components of the stator currents, not the original stator currents.

Under this operating condition, the experimental results of CMPC are shown in Fig. 7. The torque pulsation is 16%, the average switching frequency is 2050 Hz, and the THD of stator current is 4.29%.

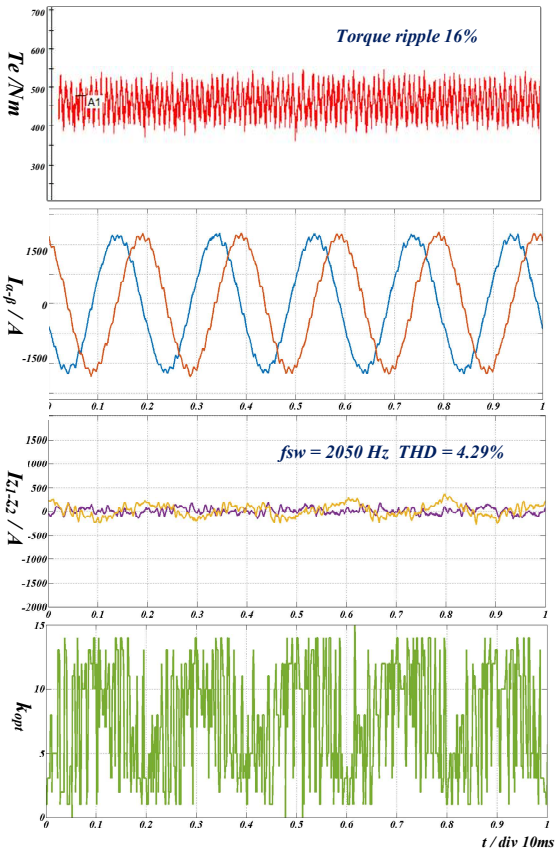

Fig. 7. Static performance of CMPC of reference current 1800 A.

Keeping the structure of the cost function and the weighting factor of the conventional MPC unchanged, the reference current reduced to 800 A. The experiment results are shown in Fig. 8. At this time, the harmonic subspace current control effect becomes worse, the torque pulsation reaches 44%, and the stator current THD reaches 24.4%. Although the torque subspace current control is basically satisfactory, due to the excessive harmonics, the system will suffer the risk of instability, which shows that the weighting factor in the traditional MPC needs to be increased at this time to strengthen the suppression ability of harmonic subspace current.

Correspondingly, the experiment results are shown in Fig. 9 when CMPC is adopted with reference current of 800 A. At this time, the harmonic subspace control effect is better, the torque pulsation is 26%, and the stator phase current THD reduces to 13.39%.

The summary of these comparison experiments is shown in Table III. Fig. 10 shows the stator current harmonic spectrum of them respectively. It can be seen from the experimental results that after the CMPC eliminates the weighting factor in the cost function, it can ensure the system obtain consistent steady-state performance under different working conditions.

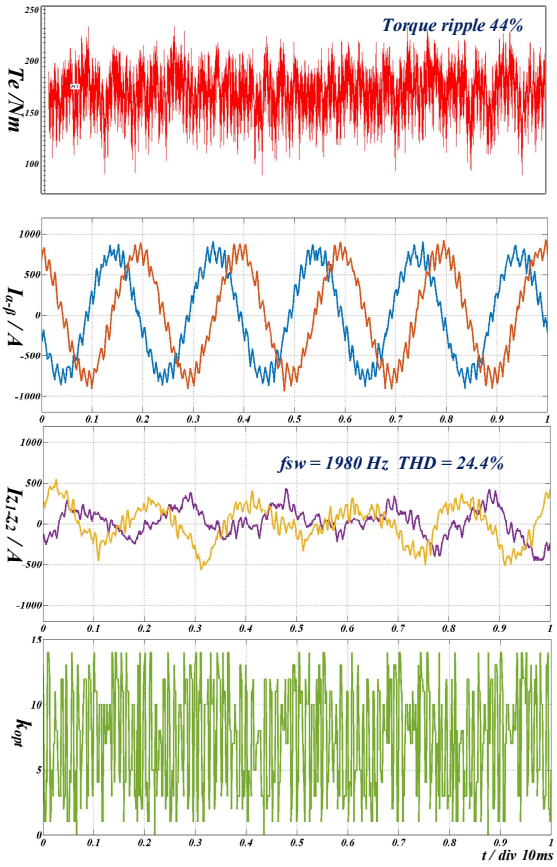

Fig. 8. Static performance of conventional MPC of reference current 800 A.

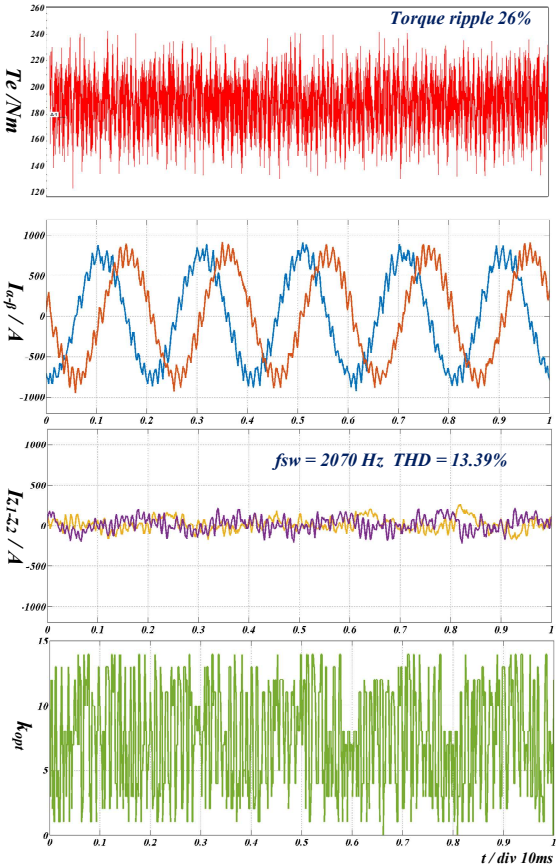

Fig. 9. Static performance of CMPC of reference current 800 A.

TABLE III
EXPERIMENT RESULTS COMPARISON

No	Method	THD/%	f_{sw}/Hz	Torque ripple/%
Fig. 6	Traditional MPC@1800A	5.20	2150	17
Fig. 7	CMPC@1800A	4.29	2050	16
Fig. 8	Traditional MPC@800A	24.40	1980	44
Fig. 9	CMPC@800A	13.39	2070	26

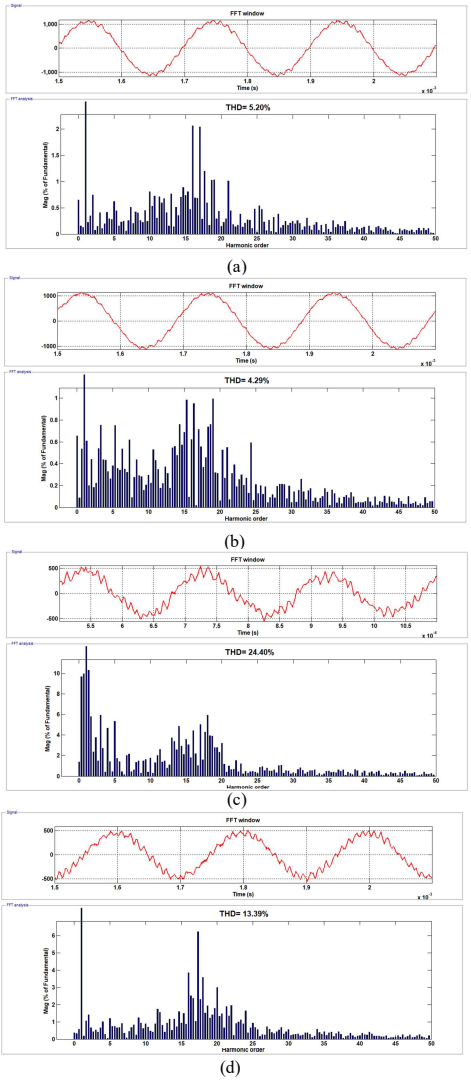

Fig. 10. Stator current harmonic spectrum related to (a) Fig. 6 (b) Fig. 7 (c) Fig. 8 (d) Fig. 9

B. Dynamic Response of CMPC and Traditional MPC

In order to verify the dynamic performance of CMPC and conventional MPC, a comparison experiment of these two control strategies under current step is conducted. Fig. 11 shows the experiment results of the dynamic response of the conventional MPC. The current reference steps from 800 A to 1800 A, and the load current tracks up the step within 3.2 ms without obvious overshoot, but the harmonic subspace current pulses more after the step, which shows that the weighting factor in the cost function cannot suppress the harmonic subspace current well at this time.

Fig. 12 shows the experiment results of the dynamic response of CMPC. The load current tracks up the step within 3.4 ms without significant overshoot. The dynamic response speed of these two MPC strategies is close, indicating that both MPC have fast dynamic response speed. The CMPC tends to stabilize the harmonic subspace current after one cycle due to the elimination of the weighting factor in the cost function, which shows that the CMPC can ensure the stability of the system operation during changing of working conditions.

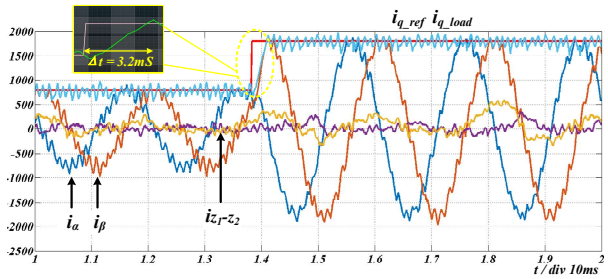

Fig. 11. Dynamic response of traditional MPC.

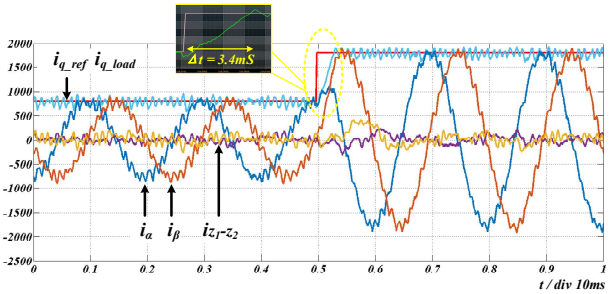

Fig. 12. Dynamic response of CMPC.

C. Fault Tolerance Verification

The fault-tolerant control capability of the CMPC proposed in this paper is verified by simulating a six-phase motor phase-loss fault by removing the PWM driving signal in one phase. Fig. 13 shows the experiment results of a_1 phase loss, from top to bottom are the stator currents of the first winding, the stator currents of the second winding, the torque subspace currents and the harmonic subspace currents, respectively. Fig.14 shows the experiment results of c_1 phase loss, and Fig.15 shows the stator current and torque waveforms before and after fault.

From the experiment results, it can be seen that by constraining the $z_1 - z_2$ current to 0, the MPC controller will select the voltage vector that generates the least harmonic current among the candidate vectors to satisfy the phase loss current constraint, and automatically switch to the fault-tolerant operation mode that satisfies the minimum stator copper loss constrain. Before and after the fault, the torque subspace current remains basically unchanged, and the phase current of the second winding increases to provide torque output. From the torque waveform in Fig. 15, it can be seen that the torque output decreases slightly and the pulsation increases after the occurrence of the phase-loss fault, but still ensures the normal operation of the system.

Besides, the traditional fault-tolerant control needs to detect which phase is open circuit. Therefore, it requires complex fault diagnosis methods. But the CMPC proposed in this paper can achieve fault-tolerant operation in case of open-circuit fault without detecting the specific open phase. Fig. 14 shows the

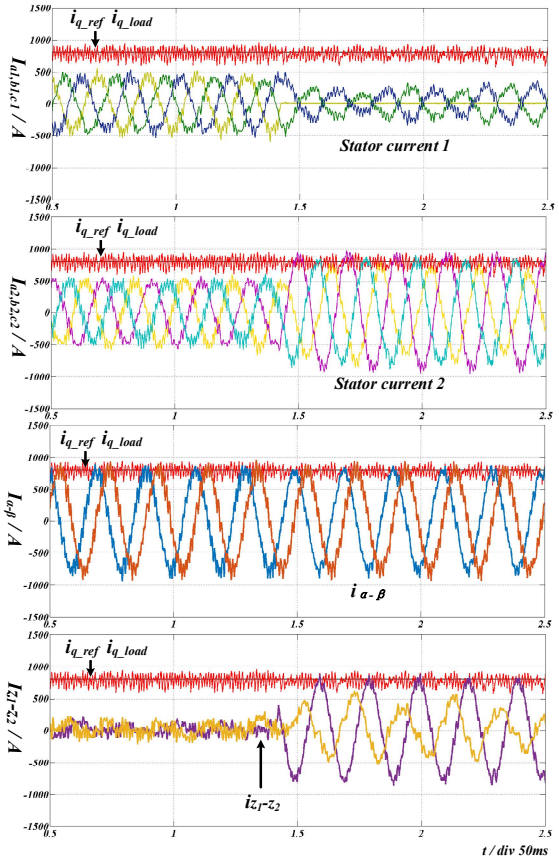

Fig. 13. Experiment results after phase a_1 open.

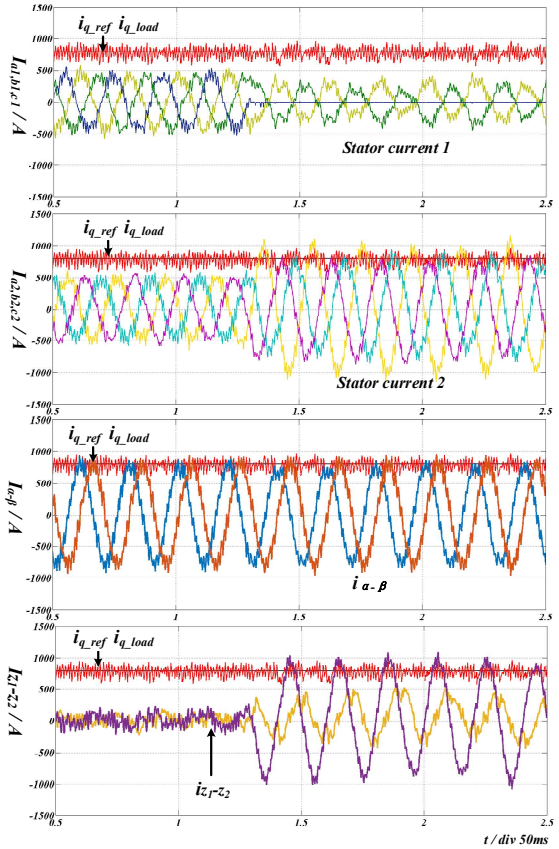

Fig. 14. Experiment results after phase c_1 open.

experiment results of CMPC when the fault phase is changed from a_1 to c_1. The experiment results show that the system can achieve the same fault-tolerant operation after the fault phase changes.

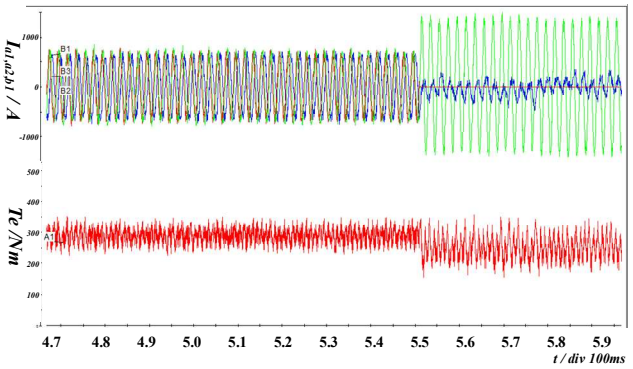

Fig. 15. Stator current and electric torque before and after fault.

V. Conclusion

For the optimal control of six-phase PMSM, a cascaded model predictive current control (CMPC) strategy with fault tolerance ability is proposed in this paper. It eliminates the influence of weighting factors on the consistency of the controller under different operating conditions. Through theoretical analysis and experiments, it is demonstrated that the CMPC proposed in this paper can achieve satisfactory static and dynamic performance under variable operating conditions in a much simpler way than the traditional methods. And it can achieve fault-tolerant control in the way of minimizing stator copper loss when any phase is open-circuit, without changing the control strategy and sensing the specific faulty phase.

References

[1] E. Levi, R. Bojoi, and F. Profumo *et al*, "Multiphase Induction Motor Drives – a Technology Status Review," *IET Electric Power Applications: Institution of Engineering and Technology*, pp. 489-516, 2007.

[2] F. Barrero, and M. J. Duran, "Recent Advances in the Design, Modeling, and Control of Multiphase Machines - Part 1," *IEEE Transactions on Industrial Electronics*, vol. 63, no. 1, pp. 449-458, 2016.

[3] A. Iqbal, and G. K. Singh, "PSO Based Controlled Six-phase Grid Connected Induction Generator for Wind Energy Generation," *CES Transactions on Electrical Machines and Systems*, vol. 5, no. 1, pp. 41-49, 2021.

[4] Y. Zhang, Z. Yin, and W. Li *et al*, "Finite Control Set Model Predictive Torque Control Using Sliding Model Control for Induction Motors," *CES Transactions on Electrical Machines and Systems*, vol. 5, no. 3, pp. 262-270, 2021.

[5] J. Rodriguez, M. P. Kazmierkowski, and J. R. Espinoza *et al*, "State of the Art of Finite Control Set Model Predictive Control in Power Electronics," *IEEE Tansactions on Industrial Informatics*, vol. 9, no. 2, pp. 1003-1016, 2013.

[6] A. A. Ahmed, B. K. Koh, and Y. I. Lee, "A Comparison Of Finite Control Set and Continuous Control Set Model Predictive Control Schemes for Speed Control of Induction Motors," *IEEE Transactions on Industrial Informatics*, vol. 14, no. 4, pp. 1334-1346, 2018.

[7] Mario Bermúdez, Cristina Martín, and Ignacio Gonzálezccrieto *et al*, "Predictive Current Control in Electrical Drives: An Illustrated Review with Case Examples Using a Five-phase Induction Motor Drive with Distributed Windings," *IET Electric Power Applications*, vol. 14, no. 8, pp. 1291-1310, 2020.

[8] W. Huang, W. Hua and Q. Fan, "Performance Analysis and Comparison of Two Fault-tolerant Model Predictive Control Methods for Five-phase PMSM Drives," *CES Transactions on Electrical Machines and Systems*, vol. 5, no. 4, pp. 311-320, Dec. 2021.

[9] I. Gonzalez-Prieto, M. J. Duran, and J. J. Aciego *et al*, "Model Predictive Control of Six-Phase Induction Motor Drives Using Virtual Voltage

Vectors," *IEEE Transactions on Industrial Electronics*, vol. 65, no. 1, pp. 27-37, 2018.

[10] Y. Zhou, and G. Chen, "Predictive DTC Strategy with Fault-tolerant Function for Six-phase and Three-Phase PMSM Series-Connected Drive System," *IEEE Transactions on Industrial Electronics*, vol. 65, no. 11, pp. 9101-9112, 2018.

[11] Y. X. Luo, and C. H. Liu, "Model Predictive Control for a Six-phase PMSM Motor with a Reduced-dimension Cost Function," *IEEE Transactions on Industrial Electronics*, vol. 67, no. 2, pp. 969 - 979, 2020.

[12] X. Zhang, and B. Hou, "Double Vectors Model Predictive Torque Control Without Weighting Factor Based on Voltage Tracking Error," *IEEE Transactions on Power Electronics*, vol. 33, no. 3, pp. 2368-2380, 2018.

[13] Y. Zhao, W. X. Huang, and X. G. Lin *et al*, "Fast Predictive Direct Torque Control of Dual Three-Phase Permanent Magnet Fault Tolerant Machine Based on Weighting Factor Elimination and Finite Control Set optimization," *Transactions of China Electrotechnical Society*, vol. 36, no. 1, pp. 3-14, 2021.

[14] M. Norambuena, J. Rodriguez, and Z. Zhang *et al*, "A Very Simple Strategy for High-Quality Performance of AC Machines Using Model Predictive Control," *IEEE Transactions on Power Electronics*, vol. 34, no. 1, pp. 794-800, 2018.

[15] Y. Zhang, B. Zhang, and H. Yang *et al*, "Generalized Sequential Model Predictive Control of IM Drives with Field-weakening Ability," *IEEE Transactions on Power Electronics*, vol. 34, no. 9, pp. 8944-8955, 2019.

[16] A. Tani, M. Mengoni, and L. Zarri *et al*, "Control of Multiphase Induction Motors with an Odd Number of Phases Under Open-circuit Phase Faults," *IEEE Transactions on Power Electronics*, vol. 27, no. 2, pp. 565-577, 2011.

[17] A. Mohammadpour, and L. Parsa, "Global Fault-tolerant Control Technique for Multiphase Permanent-magnet Machines," *IEEE Transactions on Industry Applications*, vol. 51, no. 1, pp. 178-186, 2015.

[18] Shaofeng Jia, Ziwei Liu, and Deliang Liang, "Review of Fault-tolerant Control Strategies for Multiphase Machines," *Journal of Xi'an Jiaotong University*, vol. 55, no. 6, pp. 176-184, 2021.

[19] M. Bermudez, I. Gonzalez-Prieto, and F. Barrero *et al*, "An Experimental Assessment of Open-phase Fault-tolerant Virtual-vector-based Direct Torque Control in Five-Phase Induction Motor Drives," *IEEE Transactions on Power Electronics*, vol. 33, no. 3, pp. 2774-2784, 2018.

[20] A. Kiselev , G. R. Catuogno, and A. Kuznietsov *et al*, "Finite-control-set MPC for Open-phase Fault-tolerant Control of PM Synchronous Motor Drives," *IEEE Transactions on Industrial Electronics*, vol. 67, no. 6, pp. 4444-4452, 2020.

[21] H. Guzman, M. J. Duran, and F. Barrero *et al* "Speed Control of Five-phase Induction Motors with Integrated Open-phase Fault Operation Using Model-Based Predictive Current Control Techniques," *IEEE Transactions on Industrial Electronics*, vol. 61, no. 9, pp. 4474-4484, 2014.

[22] H. Lu, J. Li, and R. Qu *et al*, "Fault-Tolerant Predictive Control of Six-phase PMSM Drives Based on Pulse width Modulation," *IEEE Transactions on Industrial Electronics*, vol. 66, no. 7, pp. 4992-5003, 2019.

[23] Wenhan Chen, Dan Sun, and Mingze Wang, "Research on Fault-tolerance Strategy Based on Model Predictive Control for Open-winding PMSM System under Open-phase Fault," *Transactions of China Electrotechnical Society*, vol. 36, no. 1, pp. 77-86, 2021.

Ling Feng was born in 1991. He received the B.S., M.S and ph.D. degrees in electrical engineering from Shanghai Jiao Tong University, Southwest Jiaotong University, China, in 2014, 2017 and 2022, respectively.

He is now a motor control R & D Engineer for CRRC ZhuZhou Institude Co., Ltd.. His research interests include multi-level convertors and model predictive control of traction system.

Zhaohui Wang received the M.S. degree in electrical engineering in 2023 from Southwest Jiaotong University, Chengdu, China, where he is currently working toward the Ph.D. degree in electrical engineering. His research interests include modeling, control, and modulation of permanent magnet synchronous motor drives.

Jianghua Feng was born in Hengyang, Hunan, China, in 1964. He received the B.S. and M.S. degrees in Electrical engineering from the Zhejiang University, Zhejiang, China, in 1989, and the Ph.D. degree in control engineering from Central South University, Changsha, China, in 2008. Since 1989, he has been with the Zhuzhou CRRC Times Electric Co., Ltd., Zhuzhou, where from 2002 to 2004, he was the Director of Technology Center, and from 2005 to 2009, he was the Technical Director of Zhuzhou CRRC Times Electric Co., Ltd., and, currently is the Chief Engineer. His research interests are in power electronics, drive control, and permanent magnet motor system. Prof. Feng was a recipient of the Mao Yisheng prize for science and technology of China, and the honorary title of Contemporary Inventor of China in 2016.

Wensheng Song (Senior Member, IEEE) received the B.S. degree in electronic and information engineering and the Ph.D. degree in electrical engineering from Southwest Jiaotong University, Chengdu, China, in 2006 and 2011, respectively. From September 2009 to September 2010, he was a Visiting Scholar with the Department of Electrical Engineering and Computer Science, University of California at Irvine, Irvine, CA, USA. From July 2015 to December 2015, he was a Visiting Scholar with the University of Alberta, Edmonton, AB, Canada. He is currently a Full Professor with the School of Electrical Engineering, Southwest Jiaotong University. His current research interests include power electronics, motor drives, railway traction drive systems, and multilevel converters.